Petroleum and Coal

Article **Open Access**

Source Parameter Imaging and 3D Euler Deconvolution method for the Determination of Geometry and Estimating Depth of Agbabu Bituminous Sand

Gideon Oluyinka Layade[1], James Adeyemo Adegoke[2], Frank Olasele Adefemi[3], Hazeez Owolabi Edunjobi[1,4]*

[1] *Department of Physics, Federal University of Agriculture, Abeokuta, Nigeria.*
[2] *Department of Physics, University of Ibadan, Ibadan Nigeria*
[3] *CCEHRD, Olusegun Agagu University of Science and Technology, Okitipupa, Nigeria*
[4] *Department of Physics, Sikiru Adetona College of Education, Science and Technology, Omu-Ajose, Nigeria*

Received May 10, 2023; Accepted July 19, 2023

Abstract

The bituminous sands of Agbabu have been mapped using several geophysical techniques. However, many of these methods provided information about the depth to the bituminous body and basement of the study area but failed to predict the possible geometry of the body. Hence, this study aimed at determining the depth to the bituminous body along with its geometry using SPI and 3D Euler deconvolution methods. A total of 161 gravity station points data were acquired, and corrected for the effect of drift, elevation and Bouguer slab effect. The SPI showed that the depth in the range of 8 m – 31 m. The 3D Euler deconvolution method revealed the assumed geometry of the free flowing bitumen in the near surface to be a fault/contact/fracture, or crack at a depth of 9 m – 35 m. The depth estimates obtained using the SPI and 3D Euler Deconvolution methods correlates greatly. These results together with the qualitative analysis of the derivative maps revealed that the bituminous sands of the study trends in the east-west direction with the presence of a fault, contact, fracture, and/or crack.

***Keywords**: Qualitative; Bouguer; Bituminous sands; Depth; Geometry; Quantitative.*

1. Introduction

Geophysics is the study of the Earth through the measurement of its physical properties. Exploration geophysics as an applied branch of geophysics uses physical methods such as magnetics, gravity, seismic, electrical, and electromagnetic methods to infer the presence and location of minerals. Among several methods applied in survey and exploration for petroleum resources, gravity survey is among the most effective for targeting prolific basins and delineating boundaries of concealed and partially concealed structures in the early stage of exploration [1]. Gravity surveys provide measurements of variations in the earth's gravity (due to variations in density) at several locations in a region. Together with the magnetic survey, the gravity method is known as the potential field method. Potential field methods are noninvasive geophysical remote sensing techniques that can measure spatial variations of the geological subsurface in terms of mass (rock density) and magnetization distribution at the earth's surface or a few hundred meters above it [2].

Crude oil was first discovered in Nigeria in 1956 at Oloibiri in the Niger Delta by Shell-BP. Since its discovery, petroleum production and export play a dominant role in Nigeria's economy and account for about 90% of Nigeria's gross earnings [3]. Due to the country's overreliance e on crude oil, and owing to the need for diversification, in recent years, the federal government through the ministry of mines and steel development has started exploring other mineral alternatives to crude oil. One of the minerals found in abundance in Nigeria is Bitumen. If exploited commercially, it represents a viable alternative to generate revenue, it will equally help reduce the reliance on imported bitumen for road construction purposes and will ultimately lead to the creation of jobs thereby improving the quality of life of the citizenry.

Bitumen is a viscous material consisting of a wide range of high molecular weight hydrocarbons represented by asphaltenes, resins, and aliphatic hydrocarbons. The primary use of bitumen is in road construction, where it is used as the binder mixed with particles to create bitumen concrete. It is equally used for waterproofing products, including the production of roofing felts and for sealing flat roofs. The bitumen deposit in Nigeria is estimated at 42.47 billion tonnes in reserve and it is found in the coastal belts of the South-Western part of the country, the deposit covers about 120-140 kilometers in the east-west direction and about 4-6 kilometers in the north-south direction with most of the reserves in Ondo state [4- 6].

The presence of bitumen in Agbabu, Ondo State has long been established in literature to be a near-surface occurrence and appears free-flowing liquid at ambient temperatures [7-10]. Previous studies carried out in Agbabu have been aimed at determining the locations of bitumen-saturated sands and the depth of the source of bitumen using various methods. In 2020 ground magnetic, Horizontal Electrical Profiling and VES were employed to determine the depth of bitumen [11] while VES was used in determining the depth to the source of bitumen in Agbabu [7,10]. Other studies focused on the geochemical and sedimentological characterization of the bituminous sands of the study area [6,10,12].

In estimating the depth of potential field sources, several estimation methods can be applied. These include 3-D Euler analytic signal, 3D Euler, Source Parameter Imaging (SPI), Half-Width and Werner deconvolution methods amongst others [13-14]]. This research aimed at evaluating the location and depth of Bitumen in the near-surface as well as to determine its probable geometry using gravity data while contributing to existing literature on Agbabu's bitumen.

2. Description and geology of the study area

Agbabu is a small town with a population of approximately 8611 located in Ondo state, Southwestern Nigeria. It is located between Ore to its north and Okitipupa to the south. It falls within the sedimentary terrain of the Dahomey basin of southwest Nigeria [7,15]. The Dahomey Basin evolved during the rifting period in the late Jurassic to early Cretaceous periods, with a Cretaceous sediment to recent sediment thickness of approximately 3000m [12,16]. The basin is known to contain several minerals such as kaolin, gypsum, limestone, bentonite, phosphate, silica sand, bitumen, gemstones, feldspar, and granite. Because of reported occurrences of bitumen deposits, the Dahomey Basin has been of geological interest and as such constitutes a viable economic hydrocarbon system [12,16]. The study area is limited to the geographical grids of latitude 6° 35' 23.91'' and 6° 35' 35.24''N and longitude 4° 49' 57.11'' and 4° 50' 14.41''E.

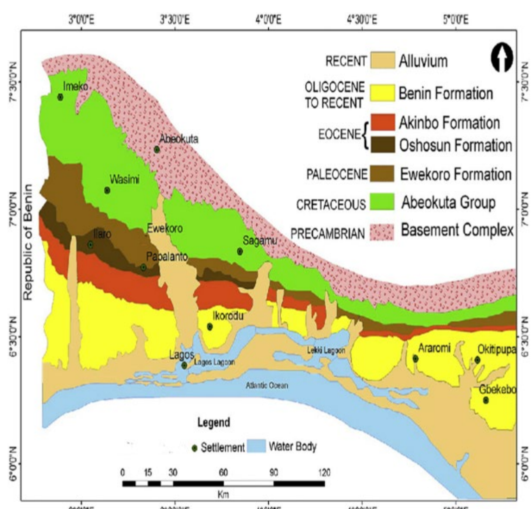

Figure 1. Geological map of the eastern Dahomey Basin Nigerian (modified after [17])

3. Materials and method

The Lacoste & Romberg gravimeter was used to acquire ground gravity data. For this survey, the Model G309 Lacoste Romberg gravimeter (with a calibration factor of 1.070120) was employed. The model G309 Lacoste & Romberg gravimeter is an unstable gravimeter that operates with a zero-length spring. Relative gravimeters are a sensitive and spring-based instrument which measures local variations in gravity reading which results from a change of mass in the subsurface as the location changes. The principle is that the changes in gravity will bring about a change in the weight of fixed mass. Therefore, the length of the spring will differ slightly with the change of location. This extension is then displayed through a suitable optical, electrical, or mechanical amplification with high precision. The gravimeter is powered using a rechargeable cell. The gravimeter has a concave aluminum metal base plate on which it is placed and adjusted before readings were taken.

Before gravity reading was taken the counter reading of the gravimeter was first determined. This was done by consulting the instruction manual of the gravimeter. The counter reading is tied to the value of the latitude at the location of the study. The counter reading was adjusted to 1550 since the survey was carried out within latitude 6^{o}. The counter reading was adjusted using the *Nulling Dial* on the gravimeter. As the gravimeter is unstable, before readings are taken the gravimeter must be constantly adjusted and stabilized. This is achieved by employing the cross-level adjustment and long-level adjustment dial on the gravimeter.

A suitable base station was selected to correct for instrument drift brought about by expansion of the elastic components of the gravimeter. The elevation, latitude and longitude, necessary for effecting needed gravity corrections, was obtained by means of a handheld, battery powered GPS while a digital clock was used to measure time which was used to correct for instrument drift.

3.1. Data acquisition

Ground gravity data was acquired across 161 data points covering eight traverses. The survey was carried out in the East-West direction. Along each traverse, the inter-station spacing adopted for this study was 25 m while the inter-traverse spacing adopted was 50 m.

3.2. Data processing

The Microsoft excel tool and the Geosoft Oasis Montaj geophysical software were employed in the processing, analysis, and interpretation of the gravity data. The raw gravity data obtained from the survey was reduced to separate the gravitational effects of subsurface density changes from those from other sources by employing necessary gravity corrections including free air correction, bouguer correction and corrections for instrument drift, before they were imported into the software and converted into a dataset containing the longitude (X–channel), latitude (Y–channel), and Bouguer anomaly (Z–channel).

Free Air Correction: The free air correction (FAC) was derived, as a function of elevation, using the formula below

$$FAC = 0.3086h \, mGal \tag{1}$$

where h is the elevation at the station.

Bouguer Correction: The Bouguer correction (BC) like the FAC is a function of elevation. It is derived using the relation below.

$$BC = 0.04191\rho h \, mGal \tag{2}$$

where h is the elevation in meters and ρ is the density of the parent rock in Mg/m^3. For this survey, the value of ρ adopted is 2.16 Mg/m^3. This was obtained from the average density of the rocks making up the geology of the study area.

✔ D0:0	X	Y	Z	long_x	lat_y	FVD	FHD
0.0	702290	728950	-1.0214	4.49.46.70	6.35.29.01	0.0013	0.0067
1.0	702315	728950	-0.7649	4.49.47.52	6.35.29.01	0.0061	0.0032
2.0	702340	728950	-0.8059	4.49.48.33	6.35.29.01	0.0090	0.0001
3.0	702365	728950	-0.9477	4.49.49.15	6.35.29.01	0.0099	-0.0025
4.0	702390	728950	-0.8677	4.49.49.96	6.35.29.00	0.0080	-0.0061
5.0	702415	728950	-1.1383	4.49.50.77	6.35.29.00	0.0040	-0.0105
6.0	702440	728950	-1.3589	4.49.51.59	6.35.29.00	0.0014	-0.0117
7.0	702465	728950	-1.7079	4.49.52.40	6.35.28.99	-0.0006	-0.0096
8.0	702490	728950	-1.6883	4.49.53.21	6.35.28.99	-0.0088	-0.0096
9.0	702515	728950	-1.8851	4.49.54.03	6.35.28.99	-0.0187	-0.0061
10.0	702540	728950	-2.1293	4.49.54.84	6.35.28.98	-0.0142	0.0158
11.0	702565	728950	-1.2735	4.49.55.66	6.35.28.98	0.0079	0.0357
12.0	702590	728950	-0.6195	4.49.56.47	6.35.28.98	0.0383	0.0124
13.0	702615	728950	-0.6154	4.49.57.28	6.35.28.98	0.0477	-0.0334
14.0	702640	728950	-2.1812	4.49.58.10	6.35.28.97	0.0075	-0.0527
15.0	702665	728950	-3.2518	4.49.58.91	6.35.28.97	-0.0390	-0.0390
16.0	702690	728950	-3.3692	4.49.59.72	6.35.28.97	-0.0379	-0.0062
17.0	702715	728950	-3.4128	4.50.00.54	6.35.28.96	-0.0161	0.0154
18.0	702740	728950	-3.2195	4.50.01.35	6.35.28.96	-0.0089	0.0072
19.0	702765	728950	-3.0647	4.50.02.16	6.35.28.96	-0.0088	0.0000
20.0	702790	728950	*	4.50.02.98	6.35.28.95	*	*
21.0	702290	729000	-1.4352	4.49.46.71	6.35.30.64	-0.0061	0.0019
22.0	702315	729000	-1.6485	4.49.47.52	6.35.30.64	-0.0020	0.0052
23.0	702340	729000	-1.8766	4.49.48.34	6.35.30.64	-0.0025	-0.0193
24.0	702365	729000	-1.8530	4.49.49.15	6.35.30.63	0.0037	-0.0069
25.0	702390	729000	-1.8508	4.49.49.96	6.35.30.63	-0.0047	-0.0067
26.0	702415	729000	-2.3380	4.49.50.78	6.35.30.63	-0.0154	-0.0090
27.0	702440	729000	-2.2929	4.49.51.59	6.35.30.62	-0.0100	0.0069
28.0	702465	729000	-1.9688	4.49.52.41	6.35.30.62	0.0021	0.0155
29.0	702490	729000	-1.8595	4.49.53.22	6.35.30.62	0.0080	-0.0022
30.0	702515	729000	-1.8648	4.49.54.03	6.35.30.62	0.0024	-0.0138
31.0	702540	729000	-1.8226	4.49.54.85	6.35.30.61	-0.0102	-0.0007
32.0	702565	729000	-2.2752	4.49.55.66	6.35.30.61	-0.0092	0.0100
33.0	702590	729000	-1.7835	4.49.56.47	6.35.30.61	0.0068	0.0045
34.0	702615	729000	-1.7894	4.49.57.29	6.35.30.60	0.0092	-0.0033

Figure 2. Snapshot of dataset from Geosoft Oasis Montaj Software

The dataset imported into the Geosoft Oasis Montaj software was gridded using minimum curvature algorithm to generate the Bouguer gravity field, which represents the observed anomaly of the entire study area (Figure 3). The Radially Averaged Power Spectrum (Figure 4) was subsequently generated from the Bouguer gravity field to visualize shallow anomaly and deep-seated anomaly sources and to reveal possible noise levels. To accentuate high frequency/low wavelength anomaly sources while attenuating short frequency/long wavelength anomaly sources, A Fast Fourier Transform (FFT2D) Guassian filter was used to filter off regional sources by cutting off sources at 0.333 cycles/km. This regional-residual separation yielded the residual map (Figure 5).

The residual anomaly grid was subsequently filtered to yield the grid derivatives using the two -dimensional Fast Fourier Transform (FFT2D) algorithm of the Oasis Montaj software. The Analytic Signal (AS) map (Figure 10) was generated to visualize the peak of anomaly sources. Along with the AS map, the Tilt Derivative Map (Figure 13) were used to reveal geological boundaries.

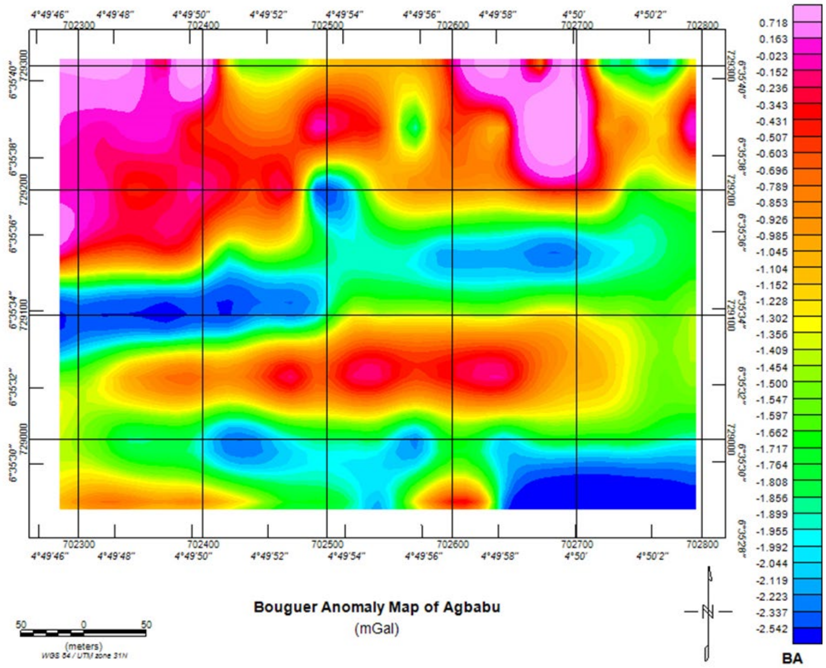

Figure 3. Bouguer anomaly map of the study area

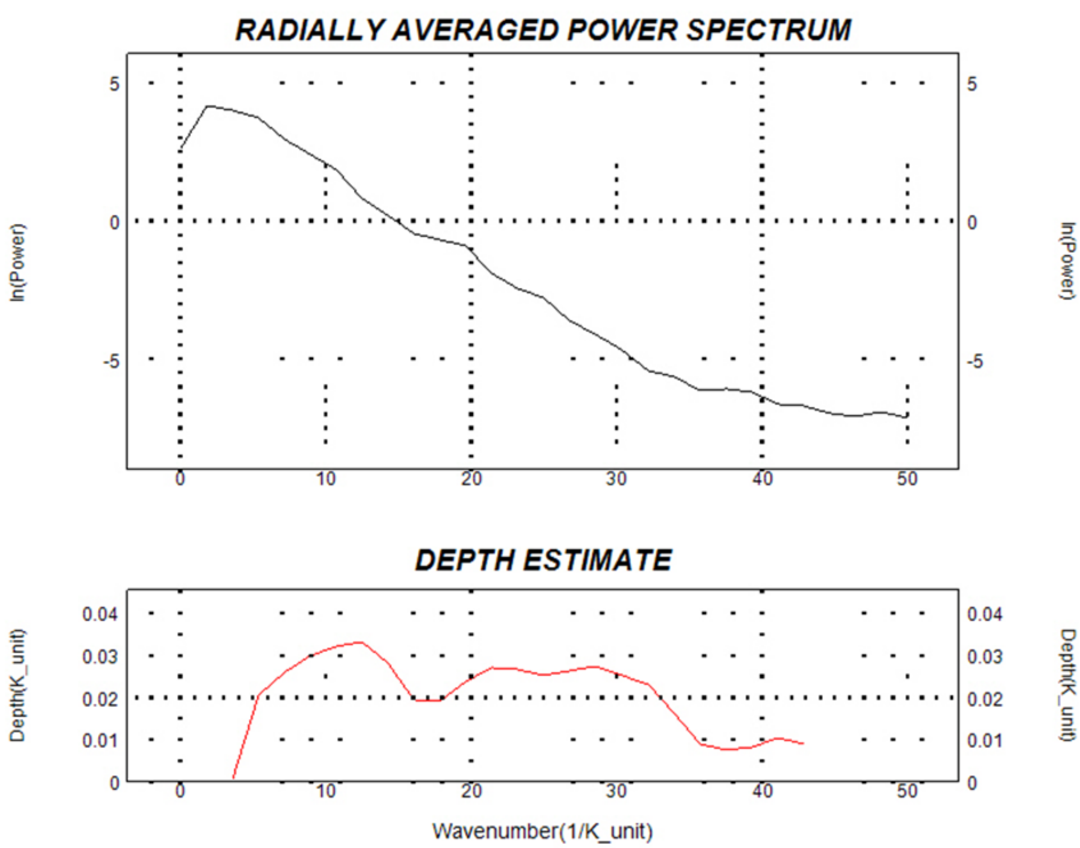

Figure 4: Radially averaged power spectrum

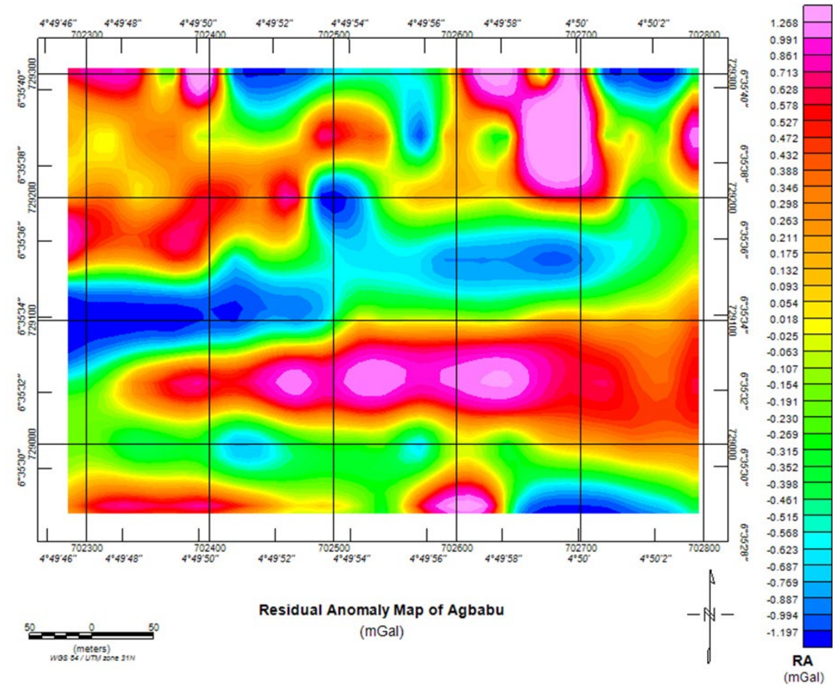

Figure 5. Residual anomaly map of the study area (Gaussian filtered at 0.333 cycles/km)

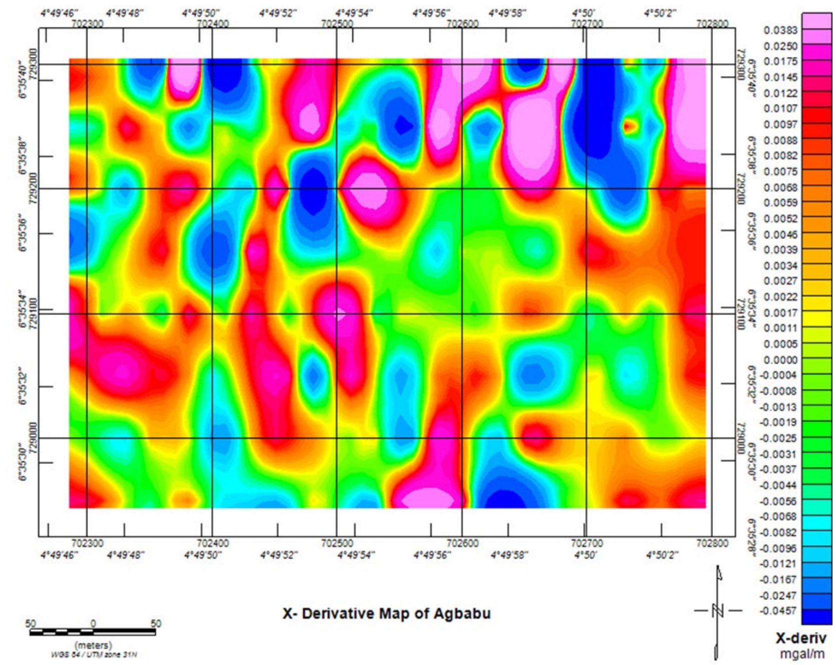

Figure 6. Horizontal X-derivative map of the study area

4. Quantitative analysis

4.1. Source parameter imaging (SPI)

The SPI also known as Local Wave Number (LWN) method was developed by [13]. Source Parameter Imaging is a useful technique because it automatically calculates source depths from gridded data, despite being susceptible to interference and noise effects. The SPI method has an advantage over Euler deconvolution or spectral depths in that there is no moving data window and the computation time is relatively short. Furthermore, noise errors can be reduced by carefully filtering the data before calculating depth. The removal of noise was achieved by removing regional anomaly sources from the total gravity field.

Before the SPI method of depth estimation can be applied, there is need to derive the following: The horizontal derivative in the X- and Y- direction (Figures 6 and 7), the vertical derivative (Figure 8), the tilt derivative (Figure 13) and the horizontal gradient of the tilt derivative (Figure 11). The SPI method utilizes an extension of complex analytic signal to estimate source depth of potential fields [18-19]. The method, developed by [14], involves applying the relationship between source depth and local wave number (K) of the potential field.

According to [20], The analytic signal $A_1(x,z)$ is defined as:

$$A_1(x,z) = \frac{\partial \varphi_{(x,z)}}{\partial x} - j\frac{\partial \varphi_{(x,z)}}{\partial z} \quad (3)$$

where $\varphi_{(x,z)}$, the magnitude of the anomalous total gravity field is, j is the imaginary number, and x and z are Cartesian coordinates for the horizontal and vertical directions respectively.

The horizontal and vertical derivatives which comprises the real and imaginary parts of the 2D analytical signal are related by;

$$\frac{\partial \varphi_{(x,z)}}{\partial x} \leftrightarrow j\frac{\partial \varphi_{(x,z)}}{\partial z} \quad (4)$$

where ↔ denotes a Hilbert transformation.

The local wave number K_1, according to [20], is defined as;

$$K_1 = \frac{\partial}{\partial x} tan^{-1} \frac{\partial \varphi}{\partial z} \Big/ \frac{\partial \varphi}{\partial x} \quad (5)$$

Therefore, the analytic signal could be defined as a second order derivative $A_2(x,z)$, where

$$A_2(x,z) = \frac{\partial^2 \varphi_{(x,z)}}{\partial z \partial x} - j\frac{\partial^2 \varphi_{(x,z)}}{\partial^2 z} \quad (6)$$

This will further give rise to second wave number, K_2, defined as;

$$K_1 = \frac{\partial}{\partial x} tan^{-1} \frac{\partial^2 \varphi}{\partial z^2} \Big/ \frac{\partial^2 \varphi}{\partial z \partial x} \quad (7)$$

The SPI map (Figure 11) of the study area was developed to reveal the depth of anomalous gravity sources.

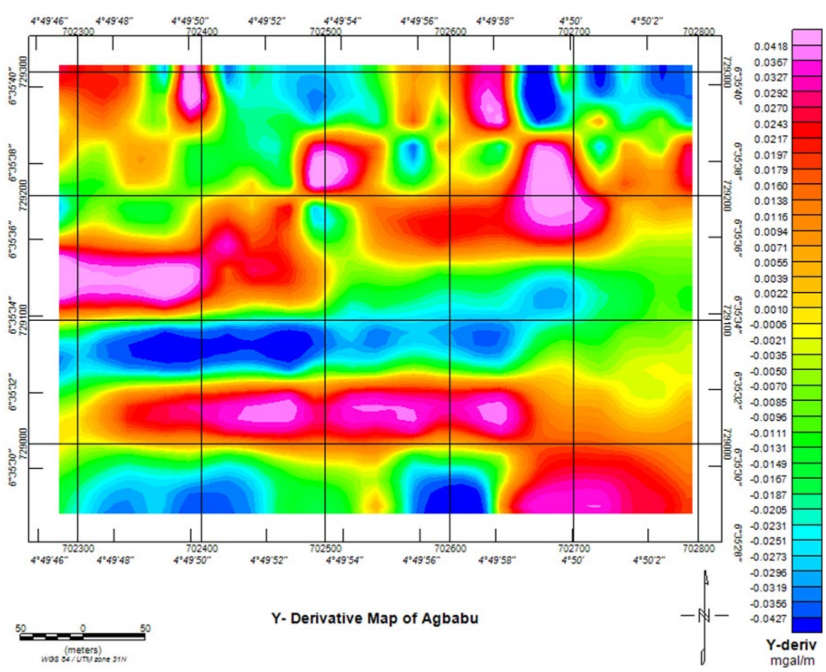

Figure 7. Horizontal Y-derivative map of the study area

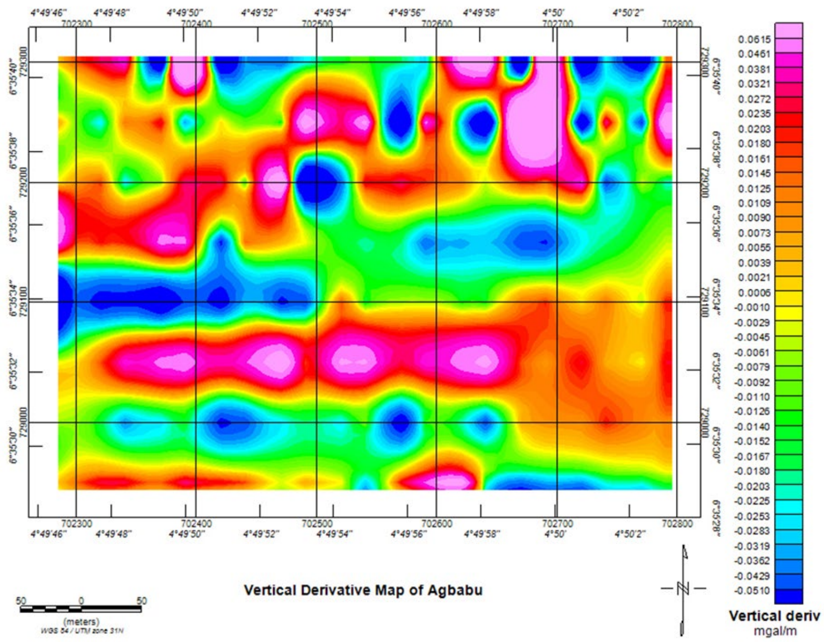

Figure 8. Vertical derivative map of the study area

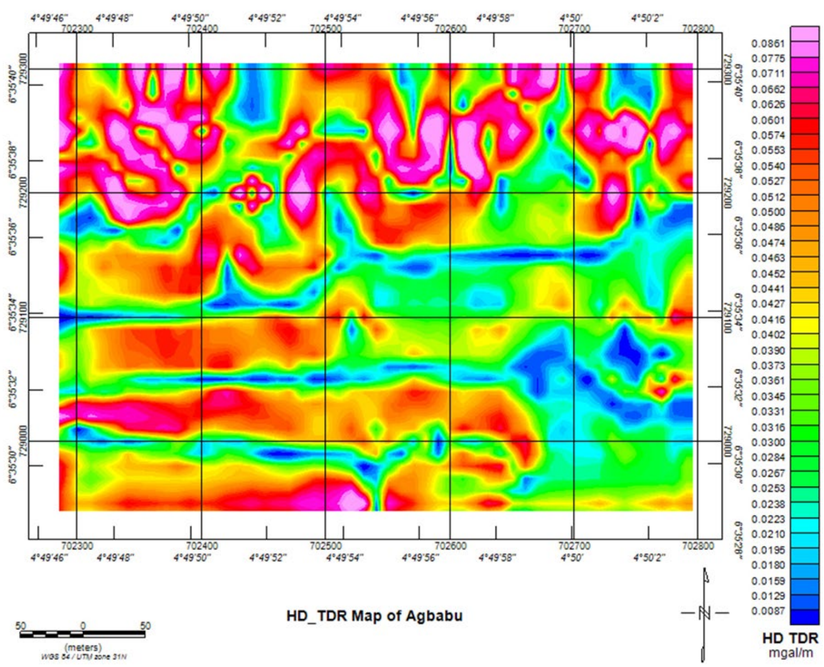

Figure 9. Horizontal derivative of tilt derivative map of the study area

4.2. The 3-D Euler deconvolution

The 3-D Euler deconvolution method was used to estimate the depth to the basement of anomalous density present in the study area.

The Euler's homogeneity equation, which connects the potential field and its gradient components to the source location and can be interpreted as a Structural Index (SI), serves as the foundation for the standard 3-D Euler deconvolution method [21]. For a source of a given geometry, The SI is assumed to be an exponential factor that represents the rate at which the potential field decays with distance.

The Standard 3D form of Euler's equation is defined as;

$$(x_i - x_o)\frac{\partial F}{\partial x} + (y_i - y_o)\frac{\partial F}{\partial y} + (z_i - z_o)\frac{\partial F}{\partial z} = \eta(b - Fi) \quad (9)$$

The measuring point's coordinates are x, y, and z; x_o, y_o, and z_o are the coordinates of the source location, whose total field is detected at x, y, and z; b is a base level; SI is the structural index (SI) and F is the total potential field. The SI which corresponds to different source geometry, as proposed by [22] for potential field measurements. The data collected was tested for different source geometries i.e fault, horizontal cylinders, and spheres which corresponds to structural indices 0, 1, and 2 respectively.

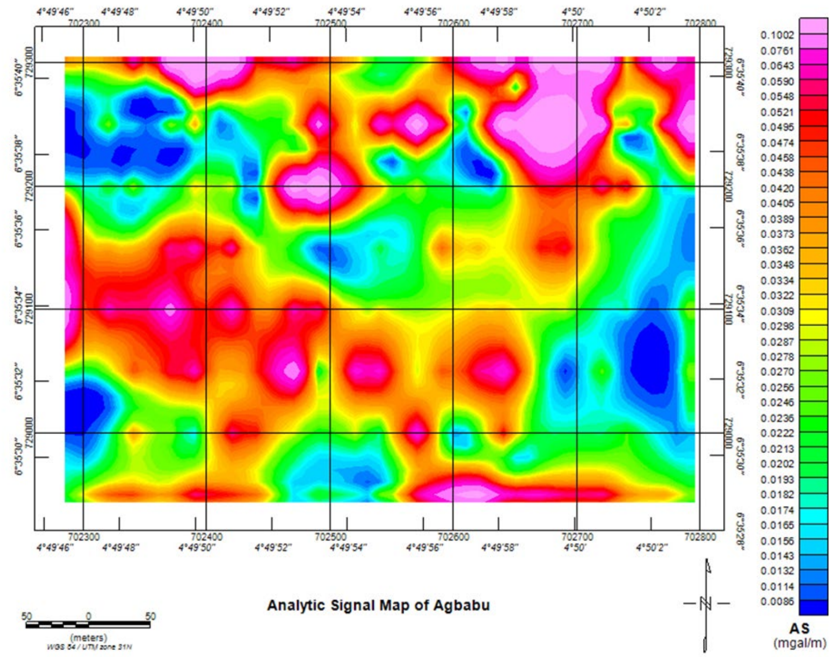

Figure 10. Analytic signal map of the study area of the study area

5. Interpretation of result

5.1. Qualitative interpretation

The digitized grid of the total gravity anomaly is as presented in Figure 2. The range of gravity values observed on the total field is -2.542 mgal to 0.718 mgal. Region of relatively high-density anomaly (Red and Pink Regions) can be observed in the north of the study area with little patches of intermediate and low gravity anomalies (represented by the green and blue region). Relatively high density contrast is equally observed trending in the east west direction in the central part of the study area. Region of low density anomaly can be observed in the SSE of the study area and trending in the East – West direction. Regions of low-density anomaly may represent entrapments of bitumen near the surface.

The bouguer gravity field contains anomalies that are near surface and those due to regional sources. Before any meaningful interpretation of data can be done, it is important to filter off regional anomaly sources from the field to accentuate shallow anomaly sources. This was accomplished by generating the Radially Averaged Power Spectrum (RAPS). The RAPS (Figure 4) is useful for visualizing deep-seated and shallow potential field sources as well as to visualize possible noise levels. Regional anomaly sources with frequency of 0.333 cycles/km were observed and filtered off using a Guassian filter. This filter accentuated shallow anomaly features while attenuating regional sources otherwise referred to as noise herein.

The Residual anomaly map (Gaussian filtered at 0.333 cycles/km, Figure 5), with an anomaly range of -1.197 mgal to 1.268 mgal, accentuated shallow anomalies that were obscured by regional sources as observed by some blue patches made visible in the northern part of the study area. Similarly, the blue region formerly observed trending in the east-west direction in the south of the study area has been reduced to noise. The blue regions, corresponding to regions of low gravity anomaly are likely area with fault lines or dikes which would be suitable entrapments for the viscous bitumen in the near subsurface.

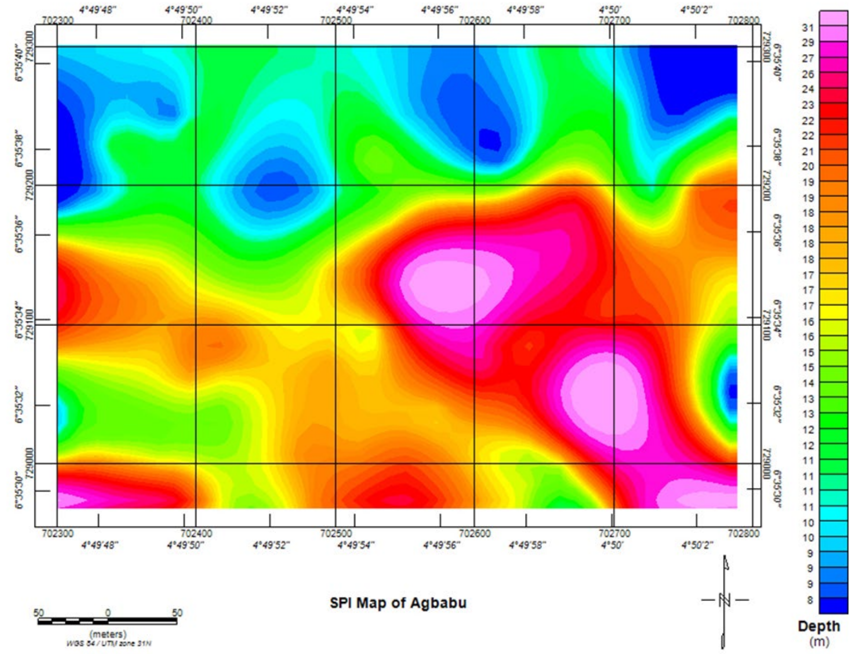

Figure 11. SPI map of the study area

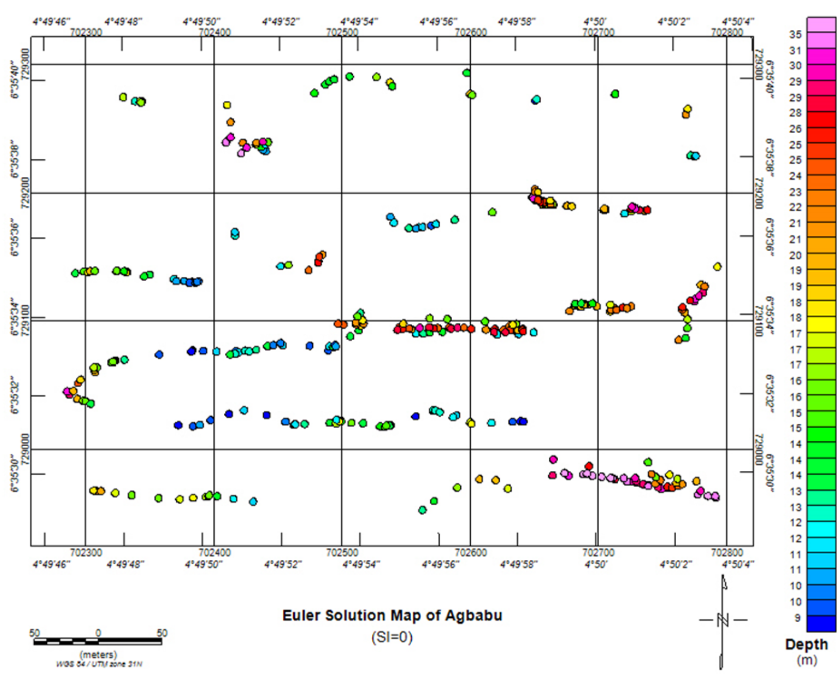

Figure 12. Euler solutions plot of the study area (SI=0)

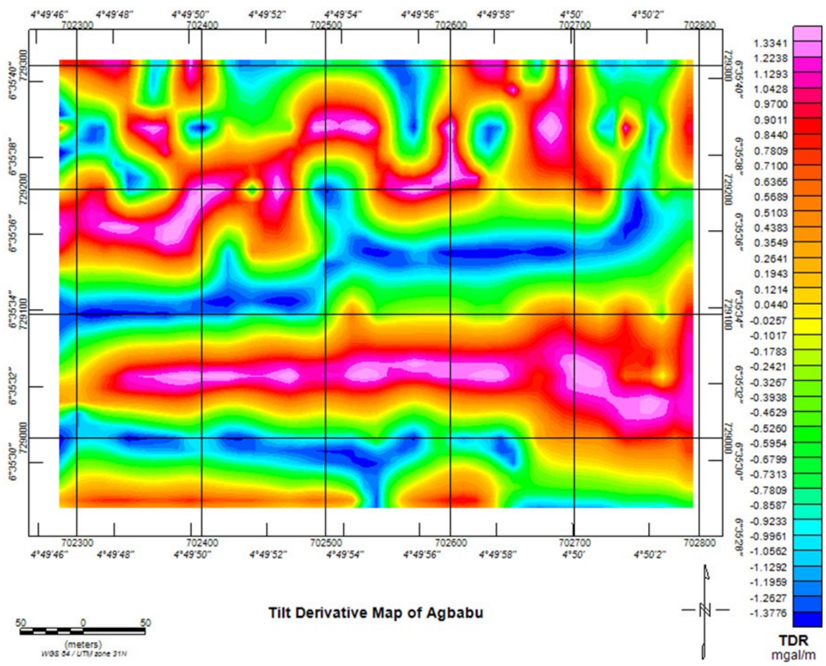

Figure 13. Tilt derivative map of the study area

In order to detect the main geologic structures and alignments in the visual interpretation of both gravity and magnetic data, edge detection techniques are routinely used [23]. The alignment of anomalies provide important information for structural analysis although it remains to be determined if the structural feature is a fault, fold or other structures. The Tilt Derivative (TDR) method was used to enhance source edges and reveal linear trends. The TDR map (Figure 13) reveals linear trends in the east-west direction. This trend might be representative of the mineralization of the study area.

The analytic signal map (Figure 10) reveals high analytic signals that ranged from 0.04 mgal/m to 0.1 mgal/m as observed in the western, northeastern and in patches in the south of the study area (denoted by the red and pink region). The area with high analytic signals like corresponds to area with high density contrasts or peaks of gravity anomaly. Regions with low analytic signals are equally observed in blue patches all over the study area.

5.2. Quantitative interpretation

5.2.1. Source parameter imaging

The SPI map of the area is presented in Figure 8. The SPI reveals a depth estimate of 8 m to 31 m. The result obtained showed that the depth to bitumen sources are shallow or near surface and this agrees with depth estimates from previous studies in Agbabu.

5.2.2. 3-D EULER deconvolution method

The 3-D Euler deconvolution method was used to estimate the depth to the basement of anomalous density present in the study area. The data collected was tested for different source geometries i.e fault, horizontal cylinders, and spheres which corresponds to structural indices 0, 1, and 2 respectively. Only the Euler solution corresponding to source geometry of faults (SI=0) (Figure 12) can be used to make meaningful geologic interpretations as the clustering is not spurious unlike that corresponding to spheres and cylinders. The data clustering confirms that the geologic structure that appears to correspond to the low-density contrast observed trending east-west in the study area is a fault. The presence of a fault will serve as conduits or entrapments for the viscous bitumen found in the near surface.

The Euler solutions map shows a depth range of 9 m – 35 m. Agbabu bitumen was found to be near surface occurrence with depths ranging from 0.5 m to 50m. In-situ investigation of some regions reveals bitumen on the surface [8,10]. This adds credence to the depth estimate obtained from the SPI and 3D-Euler deconvolution.

6. Conclusion

High-resolution gravity data in the study area in Agbabu was acquired, processed, analyzed, and interpreted qualitatively and quantitatively to reveal subsurface geologic features. Qualitative interpretations clearly show variations in the density of subsurface bodies which is most definitely due to the presence of low density materials in the study area. Similarly, derivatives map clearly reveal well defined geologic boundaries indicating heterogeneity of subsurface density materials.

The SPI method and 3D Euler deconvolution method were used to estimate the depth of anomaly sources in the entire study area. The range of values obtained clearly reveals that the anomaly is a near surface anomaly as the depth obtained is within a range of 8 m – 35 m.

References

[1] Zhang M, Qiao J, Zhao G, Lan X. Regional gravity survey and application in oil and gas exploration in China. China Geology, 2019; 2(3): 382–390.

[2] Fairhead JD, Odegard ME. Advances in gravity survey resolution. Leading Edge, 2002; 21: 36–37.

[3] History of the Nigerian Petroleum Industry: (www.nnpcgroup.com/NNPC-Business/Business-Information/Pages/Industry-History.aspx, accessed October 20, 2020).

[4] Ojeyemi MO, Akintomiwa OE, George OA, Hassan OB. The performance of Agbabu natural bitumen modified with polyphosphoric acid through fundamental and Fourier transform infrared spectroscopic investigations. Case Studies in Construction Materials, 2016; 5: 39-45.

[5] Lawal KA. Reconciling and Improving the Volumetrics of Nigerian Heavy Oil and Bitumen resources. In: SPE (Society of Petroleum Engineers), In: Nigerian Annual International Conference And Exhibition (Paper 150802). Abuja, Nigeria. 30 July–3 August, 2007.

[6] Akinmosin A. Characterization of a bitumen seepage in Eastern Dahomey Basin, SW, Nigeria. Advances in Applied Science Research, 2012; 3(4): 2078-2089.

[7] Ako BD, Alabi AO, Adegoke OS, Enu EI. Application of Resistivity Sounding in the Exploration for Nigeria Tar Sand. Energy and Exploitation 1983; 2(2): 155-164.

[8] Alagbe OA. (2020). Delineation of Bitumen Saturated Zones in Agbabu, Southwestern Nigeria, Using an Integrated Geophysical Methods. Journal of Energy and Natural Resources, 2020; 9(3): 88-97.

[9] Ogiriki, S, Agunloye, M, Gbadamosi, A. & Olafuyi, A. Exploitation Of Bitumen From Nigerian Tar Sand Using Hot-Water/Steam Stimulation Process. Petroleum and Coal. 2018; 60:217-224.

[10] Adeyemi GO., Akinmosin AA., Aladesanmi AO, Badmus GO. Geophysical and Sedimentological Characterization of a Tar Sand Rich Area in South-western Nigeria. Journal of Environment and Earth Science, 2013; 3(14):71–84.

[11] Alagbe OA. Delineation of Bitumen Saturated Zones in Agbabu, Southwestern Nigeria, Using an Integrated Geophysical Methods. Journal of Energy and Natural Resources, 2020; 9(3): 88-97.

[12] Ogala JE, Kalaitzidis S, Christanis K, Omo-Irabor OO, Akinmosin A, Yusuf CU, Pasadakis N, Constantinopoulos, M, Papaefthymiou H. Geochemical and organic petrological study of bituminous sediments from Dahomey Basin, SW Nigeria. Marine and Petroleum Geology, 2019; 99:577–595.

[13] Thurston JB, Smith RS. Automatic Conversion of Magnetic Data to Depth, Dip, and Susceptibility Contrast Using the SPITM Method. Geophysics, 1997; 62:807-813.

[14] Layade G, Adewumi O, Makinde V, Bada B. Application of Gravity Survey for the Investigation of the Presence and Depth of Iron- Ore Deposit. Petroleum and Coal, 2021 63:577 - 588.

[15] Akinmosin A, Olabode OT. Bassey, CE. Provenance Study Of Bituminous Sands In Eastern Dahomey Basin Sw Nigeria Based On Heavy Mineral And Quartz Varieties. Ife Journal of Science, 2005; 7. (1): 123-130.

[16] Nton ME, Ikhane PR, Tijani MN. Aspect of rock-eval studies of the maastrichtian-eocene sediments from subsurface, in the eastern Dahomey basin southwestern Nigeria. European Journal of Scientific Research, 2009; 25(3), 417–427.

[17] Gebhardt H, Adekeye O, Akande SO. Late Paleocene to Initial Eocene Thermal Maximum (IETM) foraminiferal biostratigraphy and paleoecology of the Dahomey Basin, southern Nigeria. Jahrbuch der Geologischen Bundesanstalt, 2010; 150:407-419

[18] Nwosu OB. Determination of Magnetic Basement Depth over Parts of Middle Benue Trough By Source Parameter Imaging (SPI) Technique Using HRAM. International Journal of Scientific and Technology Research, 2014; 3(1): 262-271.

[19] Edunjobi H, Layade G, Falufosi M, Olurin O. Lineament and Depth Evaluation of Magnetic Sources in a Geological Transition Zone of Abeokuta and its environs, Southwestern Nigeria. Petroleum and Coal, 2021; 63:548-560.

[20] Nabighian MN. The analytic signal of two-dimensional magnetic bodies with polygonal cross-section — Its properties and use for automated anomaly interpretation: Geophysics, 1972; 37:507–517.

[21] Thompson DT. EULDPH: A new technique for making computer assisted depth estimates from magnetic data: Geophysics, 1982; 47:31–37.

[22] Reid AB, Allsop JM, Granser H, Millet AJ, Somerton IW. Magnetic Interpretation in three dimensions using Euler deconvolution: Geophysics, 1990; 55:80–91.

[23] Blakely RJ, Simpson RW. Approximating Edges of Source Bodies from Magnetic or Gravity Anomalies. Geophysics, 1986; 51:1494-1498.

To whom correspondence should be addressed: Dr. Gideon Oluyinka Layade, Department of Physics, Federal University of Agriculture, Abeokuta, Nigeria; e-mail: layadego@funaab.edu.ng